ACOUSTIC NOISE ANALYSIS OF MULTIPLEXED STRATEGIES IN MULTI-OUTPUT CONVERTERS FOR INDUCTION COOKTOPS

P. Guillén*, H. Sarnago, O. Lucía, J. M. Burdío

Department of Electronic Engineering and Communications, University of Zaragoza,
C/ María de Luna, 1, 50018 Zaragoza, Spain

*Corresponding author: Pablo Guillén, Department of Electronic Engineering and Communications, University of Zaragoza, C/ María de Luna, 1, 50018 Zaragoza, Spain. Phone: +34 876 555318; Fax: +34 976 762111; E-mail: pguillenm@unizar.es.

ABSTRACT

Recent developments in domestic induction heating seek to increase the cooking surface flexibility while maintaining cost-effective implementations. In order to do so, the interconnection of classical topologies or the optimized design of new ones is being prospected. This approach usually leads to a higher complexity in the power control strategies. Thus, multiplexed load power control is used due to its versatility with the different topologies. Despite the advantages of this technique, power variations over the different pots generate a change in the forces between those and the inductors that might generate acoustic noise. This paper analyses multiplexed load power control and its restrictions and presents a modulation strategy based on switching frequency and duty cycle variation that allows a soft-transient load activation and deactivation, reducing the generated acoustic noise.

KEYWORDS

Power control, Acoustic noise, Home Appliances, Induction Heating

1. INTRODUCTION

Induction heating (IH) [1] presents remarkable advantages in domestic applications in terms of efficiency, cleanliness, and fast heating, that result in a market-leading position. In addition, in order to improve the user experience, the design trends of the induction hobs move towards systems with greater flexibility [2] that allow the use of any number of pots, independently of their shape or position on the countertop (Fig. 1).

Optimized power converter topologies have been proposed to strike a balance between the functionality of countertops and their industrialization process by reducing the number of power devices on flexible cooking surfaces [3-5]. This design trend is usually paired with a decrease in the number of degrees of freedom to control each individual inductor (IH load).

In this way, multiplexed strategies, or low-frequency pulse density modulation (LF-PDM) strategies, appear as appropriate solutions to manage a variable number of loads. Therefore, they are normally considered the main power-control methods in the inverter design, and are evaluated as an indicator of the electronic stage flexibility.

However, in order to propose a feasible multiplexed strategy several restrictions have to be addressed in terms of electromagnetic compatibility (EMC) regulations and good user experience, being the generated acoustic noise one of the most relevant [6, 7].

For normal operation, power stage generated noises are due to the inverter switching frequency while pot related noises depend on the mains harmonics [6]. In the case of multiplexation, converter noises are a result of the switching of the electromechanical devices [8], and pot vibration noises are a consequence of the power pulsation. Solutions have been proposed for this last case by synchronizing the activation with the lower bus voltage value [9], however this is not always possible.

The aim of this paper is to study different restrictions in the design of a multiplexed strategy for a certain induction cooktop and, more precisely, to analyze the physical principles involved

in noise generation during load activation and deactivation. This way a soft-start multiplexed strategy is to be proposed.

2. MULTIPLEXED STRATEGY EVALUATION

As aforementioned, multiplexed strategies are considered the main power-control methods independently of the topology. However, a cooktop development implies a multilevel design that includes the inductor layer and the routing path to interconnect them with the topology which generates an additional number of constraints to be taken into account.

2.1. Desired operation characteristics

The desired operating characteristics for the cooktop with any combination of pots can be divided into three levels: regulations level, performance level, and user experience level.

The first level focuses on compliance with EMC regulations, being the most relevant one referred to harmonic current emissions [10], voltage fluctuations and flicker [11], and household appliances emissions limits [12].

The second one can be summarized in high efficiency and passive components protection.

Finally, the user experience level is the most subjective one because it depends on the perception; however, the absence of acoustic noise and uneven heating, and an homogeneous boiling perception have been determined as relevant.

2.2. Cooktop integration

2.2.1. Inverter topology

The power converters commonly used for induction heating and, in particular, for the implementation of flexible surfaces are usually based on the half-bridge inverter topology. In addition, to reach a cost-effective solution, topologies with shared components reduce the number of devices. Thus a common solution is a single inverter with several loads connected by relays. However, in order to eliminate the relays, alternative topologies with similar control

possibilities and inductor connection routing have been presented [9].

2.2.2. Routing

Due to the characteristics of the topology, the inductors present a fixed current path and, therefore, they are powered by means of the same inverter. However, the number of inverters can be selected so that better performance is achieved and thus IH-loads can be distributed among them based on the inductor placement (Fig. 2). This fragmentation is to be evaluated to reach a balance between cost and flexibility.

2.3. Proposed solution

To control the power delivered to the load, the square-wave (SW) modulation strategy would be variable frequency, f_{sw}, and duty cycle, D, by its acronym VFDC [13] (Fig. 3 (a)) being both switching frequency and duty cycle common to all inductors that share the same inverter. However, load activation and deactivation will be driven by a low-frequency pulse density modulation strategy [14] (Fig. 3 (b)). This combination of modulations presents the following degrees of freedom: f_{sw}, D, T_{PDM}, $t_{on,PDM,i}$ and $\varphi_{PDM,i}$.

In order to decrease complexity while not limiting versatility, power output while the load is active would be set only by switching frequency. Therefore, duty cycle would be maintained constant and symmetrical to reach higher efficiency. The selected frequency must guarantee zero voltage switching (ZVS) in order to ensure the integrity of the converter, maximize the efficiency, and limit the voltage in the resonant capacitor. In order to reduce frequency limitations, it will be possible to deactivate the less-covered inductors, assuming that the pot is designed to allow a correct distribution of the heat.

Thus, the VFDC strategy is enough to fulfill performance level constraints while LF-PDM strategy will be used to reach an adequate user experience while complying with EMC regulations. This way, boiling perception is seen as continuous with a high multiplexation rate. As a consequence, flicker regulation is the limiting one and therefore, the appliance input power

is to be kept constant.

Considering the previous facts, single-inductor activation is to be avoided due to low power available. Thus, pot regions will be created by synchronizing the activation of the inductors under the same pot. Therefore, all inductors under the same pot share $t_{on,PDM,i}$ and $\varphi_{PDM,i}$.

With this preliminary design, in the particular case of a pot over the appliance, it is sufficient to do $t_{on,PDM,i} = T_{PDM}$ and $\varphi_{PDM,i} = 0$ and reach the target power through frequency variation, which will be equal for all the inductors.

Having solved the problem for a single pot, the multiplexed strategy is used for the case of several pots. In this way, pot activation creates a sequence of time slots with constant output power, sharing them differently among the pots depending on the activation of the inductors. Consequently, the pots are delivered higher or lower power than the target, but reaching the desired average power (Fig. 4).

Those time slots present different activation modes and, therefore, different frequencies to reach the same output power. For the cases depicted in Fig. 4, in the first one only inductors under pot 1 are active. In the second one, the same occurs for pot 2. In the third time slot, all covered inductors are active. In addition, the last two slots use the division into inverters of the cooktop so that pots that are placed over different inverters work at different frequencies.

This strategy reaches the desired operation but does not take into account the generated acoustic noise.

3. NOISE ANALYSIS

To ensure a proper user experience household equipment have to operate with reduced noise generation. Being the range of audible frequencies between 20 Hz and 20 kHz, not all frequencies are perceived with the same intensity by the human ear [15]. In this paper, the A-weighting curve, which gives a greater weighting to the frequencies between 1 and 6 kHz, is

used to estimate the level of disturbance of the produced noise.

Based on that, to solve the noise problem in normal operation, switching frequency would be over 20 kHz. In the case of several inverters working simultaneously they should use a single frequency or the selected frequencies should differ from each other at least 20 kHz to avoid producing intermodulation acoustic noise.

For the case of pot vibration during multiplexation, a more in-depth analysis is to be performed.

3.1. Theoretical approximation

Perceived vibrations can be modelled assuming that the pot behaves as an indeterminate series of linked damped systems [16], with the matrix differential equation being described as follows:

$$\mathbf{m}\frac{d^2}{dt^2}\mathbf{x} + \mathbf{c}\frac{d}{dt}\mathbf{x} + \mathbf{kx} = \mathbf{F}(t), \tag{1}$$

being **m** the mass matrix of the different systems, **c** the viscous damping matrix, **k** the matrix of elastic constants, **F** the vector of applied forces and **x** the position vector of the different systems. The step response of this system establishes that the vibration will present an exponential decay of the form:

$$\frac{d^2}{dt^2}x = k_1 \Delta\mathbf{F} \cdot e^{-\tau \cdot t}, \tag{2}$$

where k_1 is the proportionality constant which is dependent of non-modifiable parameters so is not calculated. In conclusion, the perceived noise level will be proportional to the variation of force over the pot.

Moreover, this force is the addition of the magnetic attraction over the ferromagnetic part of the pot and the repulsion due to the induced eddy currents, being the second the most relevant [17].

The force due to the induced currents is the result of application of the Lorentz forces,

$$\mathbf{F} = \mathbf{I_{ind}} \times \mathbf{B}, \tag{3}$$

where **B** is the magnetic field generated by the inductor and $\mathbf{I_{ind}}$ the current induced in the bottom of the pot.

The magnetic field generated by a loop can be calculated by the Biot and Savart equation:

$$\mathbf{dB} = \frac{\mu_0 I_o \mathbf{dL} \times \hat{\mathbf{r}}}{4\pi R^2}, \tag{4}$$

being $\mathbf{I_0}$ the current through the inductor, $\hat{\mathbf{r}}$ the unitary vector with radial direction and **dL** the differential of the length of the turn. On the other hand, the equation that describes the induced current is the following:

$$M \frac{d}{dt} i_o = i_{ind} R_L + L_r \frac{d}{dt} i_{ind}. \tag{5}$$

Combining the solutions of equations (4) and (5) into equation (3), it is obtained that the applied force will be proportional to the excitation current squared,

$$\mathbf{F} = k_2 {I_{o,rms}}^2, \tag{6}$$

being k_2 the proportionality constant. Consequently, it can be concluded that the acoustic emission will be proportional to the variation of the square of the current flowing through the inductor.

3.2. Proposed solution

As explained above, the problem arises in the activation or deactivation of the loads when using the PDM strategy, therefore, the proposed solution will be based on achieving a smooth activation and deactivation by modifying the parameters in the VFDC strategy.

In order to achieve a reduction in acoustic noise, a modulation is proposed that results in a linear variation of the force. For this, the form of the RMS current over time should be

$$I_{o,rms}(t) = \sqrt{C \cdot t}, \tag{7}$$

where C is the constant that models the slope of the curve. If the function is discretized in k

switching cycles of period $T(k)$, and taking into account that it is not possible to start the modulation with zero current,

$$I_{o,rms}(k) = \sqrt{C \cdot \sum_{1}^{k} T(k) + I_{o,rms}(0)^2}. \quad (8)$$

Therefore, C will set the switching period change rate, and the duty cycle is only used to lower the initial current and smoothen the curve.

A representative modulation can be seen in Fig. 5 for a final RMS current of 21.4 A. The selected curve slope is C = 1.5 A^2/μs and the initial current $I_{o,rms}(0)$ = 5.71 A. Those parameters lead to a 280 μs ramp duration composed of 15 switching cycles.

4. EXPERIMENTAL SETUP

In order to check the feasibility of the proposed modulation, an experimental setup that allows generating different activation slopes and measuring the noises associated with them has been built.

4.1. Power topology

The inverter topology is a resonant half-bridge based on an IGBT module connected to an inductor-IH load system, modeled as a series resistance, R_L, and inductance, L_r . In order to complete the resonant tank, a capacitor, C_r, is added in series. The values of the different parameters at resonant frequency are R_L = 2.02 Ω, L_r = 23 μH and C_r = 132 μF. The system is controlled through an FPGA that allows to program the variations of the switching frequency and the duty cycle.

4.2. Noise measurement system

The generated noise is measured through a piezoelectric element attached in vertical position to the surface of the pot as seen in Fig. 6. The voltage drop in this element varies when it is deformed, so that it is possible to detect the horizontal vibrations in the pot wall.

4.3. Signal processing

Even though voltage variation in the piezoelectric element provides enough information for a qualitative analysis of the results, in order to evaluate the level of discomfort of the user several signal processing stages are required. First of all, a low pass filter is necessary to eliminate the contributions to the signal due to the electromagnetic disturbances produced by the generated magnetic field. The cut-off frequency of this filter is set so inverter switching frequency is blocked. Secondly, an equalizer is implemented to flatten the piezoelectric frequency response so that the gain is equal for the different frequencies. Finally, an A-weighting filter is carried out in order to approximate the observed results to the human hearing.

5. EXPERIMENTAL RESULTS

Based on experimental measurements both the theoretical approximations made and the viability of the proposed solution is checked.

In order to test the theoretical approximations, pulses of different current levels have been applied to the load and piezoelectric voltage drop has been directly measured. In Fig. 7 (a), the exponential decay of the step response can be seen, as stated in equation (2) while the proportionality of the force step with the current step square proposed in equation (6) is shown in Fig. 7 (b). This last approximation can be seen to present deviations due to other forces and neglected second order effects.

Once the analytical model is proven to be accurate enough, the proposed soft-start multiplexed modulation is to be evaluated. The representative waveforms can be seen in Fig. 8. For it, a slope constant C = 0.035 $A^2/\mu s$ is selected. Starting from an initial current, $I_{o,rms}(0)$ = 5.7 A, and being the RMS current to reach the desired power 21.4 A, the total slope time is 12.12 ms and the number of switching cycles is approximately 600. In this figure, as in

simulation, a high initial current can be seen due to high frequency limitations, e.g. switching power losses, and therefore low initial switching frequency, f_{sw} = 75 kHz. Despite this, the current form greatly diminishes the perceived noise. Focusing on the piezoelectric voltage drop it can be seen that turn-on noise is greater than turn-off noise and that noise is measured during operation. This differences are due to the electromagnetic field generated by the cooktop and are greatly diminished when filtering the signal.

In Fig. 9 perceived noise, calculated after processing the piezoelectric signal, is shown. In this plot, the dependence between noise level and the modulation slope is shown. From left to right current curve slope increases, reducing the number of necessary switching cycles to reach the desired power and decreasing the ramp duration but increasing the sound pressure level. In order to reach a balance, a reference such as the maximum noise for homes seem a good approximation. However, it is necessary to take into account the power reduction these strategies involve.

6. CONCLUSIONS

In this paper, a multiplexation strategy for two pots has been proposed based on the analysis of the design constraints and the desired performance analyzing the cooktop from the topology level to the inductor distribution.

In addition, a soft-start modulation, whose purpose is to reduce the noise generated by domestic induction appliances has been presented. This modulation enables delivering high pulsating power levels without generating undesired noises.

The feasibility of the soft-start multiplexed modulation has been proved experimentally. In addition to this, it has been proven feasible to perform acoustic noise measurement by monitoring vibrations in the elements that generate it.

7. ACKNOWLEDGEMENTS

This work was partly supported by the Spanish MINECO under Project TEC2016-78358-R, by the Spanish MICINN and AEI under Project RTC-2017-5965-6, co-funded by EU through FEDER program, by the DGA-FSE, by the MECD under the FPU grant FPU17/01442 and by the BSH Home Appliances Group.

8. REFERENCES

[1] O. Lucía, P. Maussion, E. Dede and J. M. Burdío, Induction heating technology and its applications: Past developments, current technology, and future challenges, *IEEE Transactions on Industrial Electronics* **61** (2014), 2509-2520. DOI 10.1109/TIE.2013.2281162.

[2] O. Lucía, J. Acero, C. Carretero and J. M. Burdío, Induction heating appliances: Towards more flexible cooking surfaces, *IEEE Industrial Electronics Magazine* **7** (2013), 35-47. DOI 10.1109/MIE.2013.2247795.

[3] O. Lucía, J. M. Burdío, L. A. Barragán, J. Acero and C. Carretero, Series resonant multi-inverter with discontinuous-mode control for improved light-load operation, *IEEE Transactions on Industrial Electronics* **58** (2011), 5163-5171. DOI 10.1109/TIE.2011.2126541.

[4] H. Sarnago, O. Lucia, A. Mediano and J. Burdio, Efficient and cost-effective ZCS direct ac-ac resonant converter for induction heating, *IEEE Transactions on Industrial Electronics* **61** (2014), 2546-2555. DOI 10.1109/TIE.2013.2262752.

[5] F. Forest, E. Labouré, F. Costa and J.-Y. Gaspard, Principle of a multi-load/single converter system for low power induction heating, *IEEE Transactions on Industrial Electronics* **15** (2000), 223-230.

[6] M. Nakagawa and H. Yonemori, A study on the audible frequency area noise emanating from a pan when the IH cooker is fed by the power source including harmonics, *International Journal of Applied Electromagnetics and Mechanics* **59** (2019), 1421-1430. DOI 10.3233/jae-171236.

[7] H. Yonemori, A. Fujiwara, R. Maruyama and M. Kobayashi, Study on the high frequency acoustic noise and vibration of a pan generated by an IH cooker, *International Journal of Applied Electromagnetics and Mechanics* **45** (2014), 449-456. DOI 10.3233/jae-141863.

[8] E. Ramirez-Laboreo, C. Sagues and S. Llorente, A New Run-to-Run Approach for Reducing Contact Bounce in Electromagnetic Switches, *IEEE Transactions on Industrial Electronics* **64** (2017), 535-543. DOI 10.1109/TIE.2016.2605622.

[9] M. Pérez-Tarragona, H. Sarnago, Ó. Lucía and J. M. Burdío, High performance full-bridge multi-inverter featuring 900-V SiC devices for domestic induction heating applications, *EPE Journal* (2017), 1-10. DOI 10.1080/09398368.2017.1417786.

[10] IEC, IEC 61000-3-2:2014 Electromagnetic compatibility (EMC) - Part 3-2: Limits - Limits for harmonic current emissions (equipment input current <= 16 A per phase).

[11] IEC, IEC 61000-3-3:2013 Electromagnetic compatibility (EMC) - Part 3-3: Limits - Limitation of voltage changes, voltage fluctuations and flicker in public low-voltage supply systems, for equipment with rated current ≤16 A per phase and not subject to conditional connection.

[12] CISPR, CISPR 14-1:2016 Electromagnetic compatibility - Requirements for household appliances, electric tools and similar apparatus - Part 1: Emission.

[13] O. Lucía, J. M. Burdío, I. Millán, J. Acero and L. A. Barragán, Efficiency oriented design of ZVS half-bridge series resonant inverter with variable frequency duty cycle control, *IEEE Transactions on Power Electronics* **25** (2010), 1671-1674. DOI 10.1109/TPEL.2010.2042461.

[14] V. Esteve *et al.*, Improving the Efficiency of IGBT Series-Resonant Inverters Using Pulse Density Modulation, *IEEE Transactions on Industrial Electronics* **58** (2011), 979-987. DOI 10.1109/TIE.2010.2049706.

[15] V. Mellert, U. Richter, H. Møller, L. Nielsen, K. Ashihara and H. Takeshima (2003). *Precise and Full-range Determination of Two-dimensional Equal Loudness Contours*, Tohoku University, Japan.

[16] Z. Xun, L. Xiaozhen, W. Guoqiang and X. Liang, Vibration and sound radiation of Rail Transit viaduct, *2011 International Conference on Electric Technology and Civil Engineering*

(ICETCE) (2011), 937-940.
[17] C. M. Zingerli, T. Nussbaumer and J. W. Kolar, Optimizing repulsive lorentz forces for a levitating induction cooker, *2014 International Power Electronics Conference (IPEC-Hiroshima 2014 - ECCE ASIA)* (2014), 3365-3370.
[18] H. Sarnago, L. Ó and J. M. Burdío, FPGA-Based Resonant Load Identification Technique for Flexible Induction Heating Appliances, *IEEE Transactions on Industrial Electronics* **65** (2018), 9421-9428. DOI 10.1109/TIE.2018.2823687.

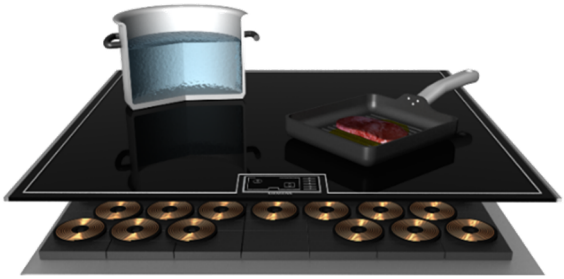

Fig. 1. Flexible cooking surface [18].

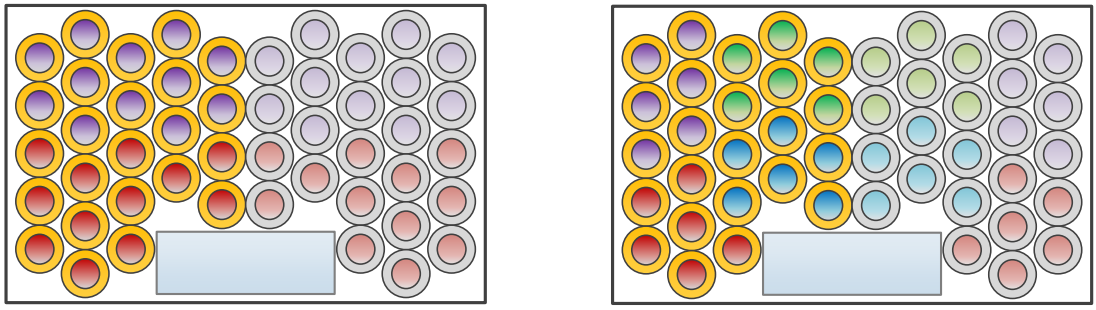

(a) (b)

Fig. 2. Flexible cooking surface inductor distribution and inverter division considering a symmetrical two phase device. Cases of two (a), and four (b) blocks per mains phase.

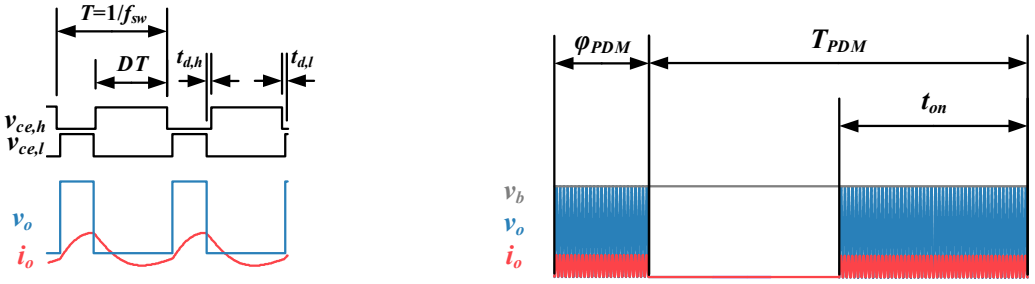

(a) (b)

Fig. 3. Main waveforms and control parameters for VFDC (a) and PDM (b) modulation strategies.

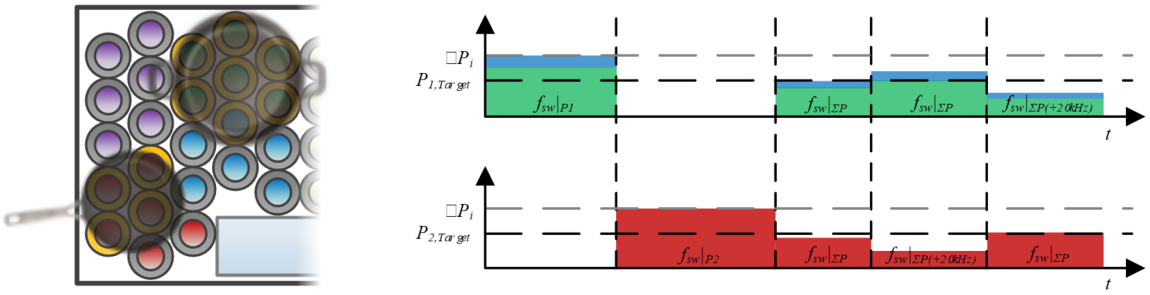

Fig. 4. Example of two pots power multiplexed strategy.

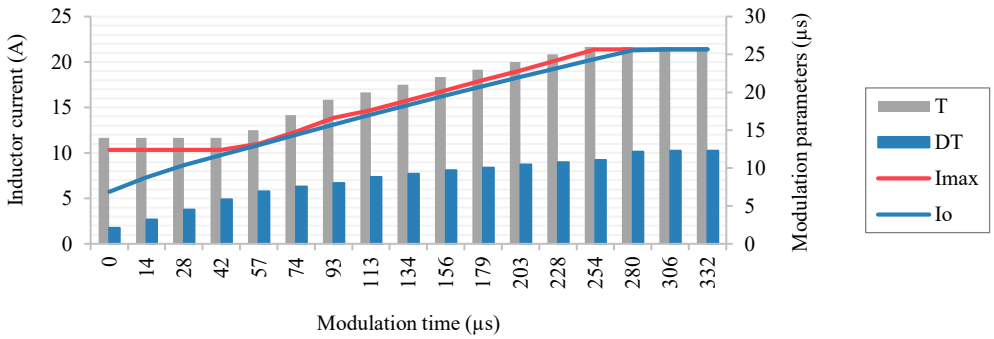

Fig. 5. Illustrative example of a solution for 1800 W output power where I_o is the goal RMS current, and I_{max} is the maximum RMS current for a certain switching frequency. Switching period, T, and on time, $D \cdot T$, are also shown.

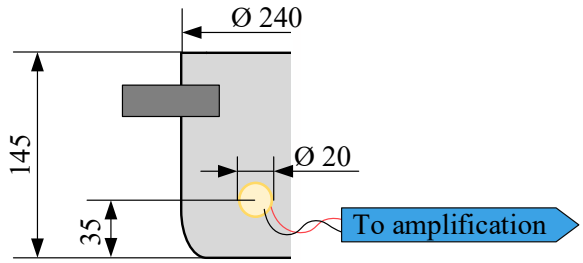

Fig. 6. Geometric details and positioning of the piezoelectric element on the pot wall. Units in mm.

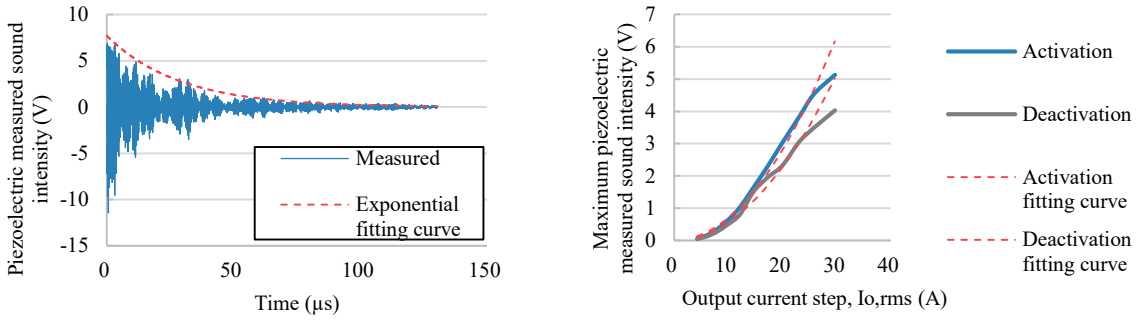

(a) (b)

Fig. 7. System response to a 30 A current step (a) and measured sound intensity for different current steps (b).

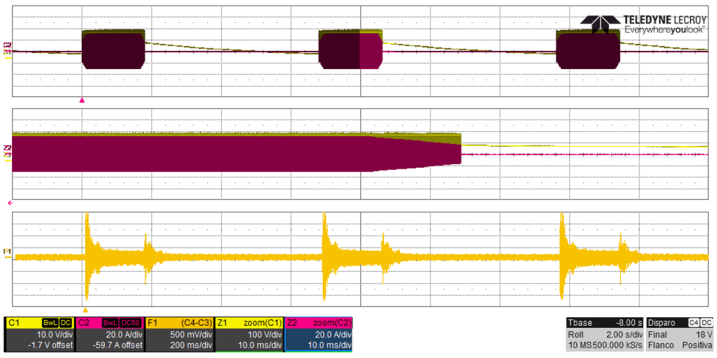

Fig. 8. Oscilloscope capture showing three power pulses, a zoomed deactivation modulation, and piezoelectric vibration measurements. Upper axis (200 ms/div) and Central axis (10 ms/div): inverter output voltage, v_o, (100 V/div, yellow), inductor current, i_o, (20 A/div, pink). Lower axis (200 ms/div): sensor output voltage, (500 mV/div, orange).

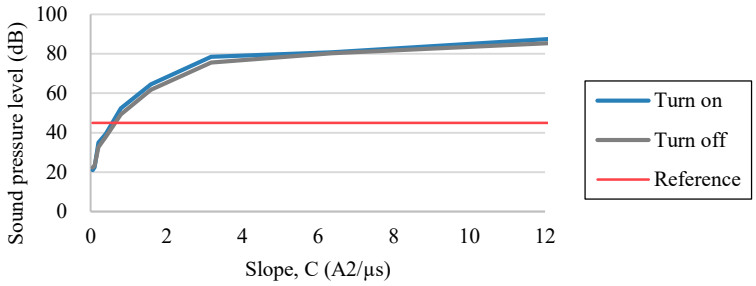

Fig. 9. Variation of acoustic noise with modulation slope for 1800 W pulsating power. Initial current, $I_{o,rms}(0)$ = 5.7 A and final RMS current of 21.4 A.